NATIONAL ADVISORY COMMITTEE FOR AERONAUTICS

TECHNICAL NOTE 2318

FULL-SCALE-TUNNEL INVESTIGATION OF THE STATIC-THRUST PERFORMANCE OF A COAXIAL HELICOPTER ROTOR

By Robert D. Harrington

Langley Aeronautical Laboratory
Langley Field, Va.

Washington

March 1951

NATIONAL ADVISORY COMMITTEE FOR AERONAUTICS

TECHNICAL NOTE 2318

FULL-SCALE-TUNNEL INVESTIGATION OF THE STATIC-THRUST PERFORMANCE OF A COAXIAL HELICOPTER ROTOR

By Robert D. Harrington

SUMMARY

An investigation to determine the static-thrust performance of a coaxial helicopter rotor having blades tapered both in plan form and thickness ratio has been conducted in the Langley full-scale tunnel. Tests of both the coaxial-rotor and single-rotor configurations were made for a range of blade-pitch setting and for a range of tip speed up to 500 feet per second. Several tests were also conducted to determine the effect of variation in directional control on the hovering performance of the coaxial rotor.

A comparison of the measured static-thrust performance of the rotor with that predicted by hovering-performance theory is also presented. Included to substantiate the comparison with hovering theory are some previously obtained static-thrust results of another coaxial rotor of higher solidity and different blade geometry. The theoretical calculations for the coaxial configurations are based on the assumption of a single rotor with a solidity equal to that of the coaxial rotor and are in good agreement with the measured results.

INTRODUCTION

A general research program to investigate the aerodynamic characteristics of several different helicopter-rotor configurations is in progress at the Langley full-scale tunnel. An investigation of a coaxial helicopter rotor, with blades tapered both in plan form and thickness ratio and representing the case of 100-percent rotor overlap, has recently been conducted as part of this program. Included in the investigation were tests to determine the performance and blade-motion characteristics of the rotor over a range of airspeed. Tests were also made with one rotor removed in order to determine the relative merits of the coaxial- and single-rotor configurations.

This paper presents the results of static-thrust measurements for both the coaxial- and single-rotor configurations along with a comparison

of these results with hovering-performance theory. Included to substantiate the comparison with theory are some previously obtained full-scale-tunnel static-thrust data for a coaxial rotor of higher solidity and with blades tapered in thickness ratio only.

SYMBOLS

b	number of blades
R	blade radius, feet
r	radial distance to blade element, feet
x	ratio of blade-element radius to rotor-blade radius (r/R)
t	blade section thickness, feet
c	blade section chord, feet
c_e	equivalent blade chord, feet $\left(\frac{\int_0^R cr^2\,dr}{\int_0^R r^2\,dr}\right)$
σ	rotor solidity $(bc_e/\pi R)$
ρ	mass density of air, slugs per cubic foot
Ω	rotor angular velocity, radians per second
T	rotor thrust, pounds
Q	rotor torque, pound-feet
C_T	rotor thrust coefficient $\left(\frac{T}{\rho(\Omega R)^2\pi R^2}\right)$
C_Q	rotor torque coefficient $\left(\frac{Q}{\rho(\Omega R)^2\pi R^3}\right)$

M	rotor figure of merit $\left(0.707 \frac{C_T^{3/2}}{C_Q}\right)$
c_{d_o}	profile drag coefficient of rotor-blade section
c_l	section lift coefficient of rotor-blade section
a	slope of section lift curve against angle of attack in radians
α_r	blade-element angle of attack measured from line of zero lift, radians $(\theta - \varphi)$
θ	blade-section pitch angle, radians
φ	inflow angle at blade element, radians $\left(\tan^{-1} \frac{v}{\Omega r}\right)$
v	induced inflow velocity at rotor, feet per second
$\delta_0, \delta_1, \delta_2$	coefficients in power series expressing c_{d_o} as function of α_r $\left(c_{d_o} = \delta_0 + \delta_1\alpha_r + \delta_2\alpha_r^2\right)$

Subscripts:

r	root
t	tip
o	profile

APPARATUS AND TESTS

The helicopter-rotor configuration tested in this investigation (rotor 1) consisted of two, 25-foot-diameter, two-blade rotors. The rotor drive mechanism consists of a pair of hubs mounted 2.33 feet (9.5 percent of the rotor diameter) apart on coaxial, dual-rotating drive shafts. The hubs were attached to their respective drive shafts by a single horizontal pin which allowed the blades to flap see-saw fashion; they were, however, rigidly restrained in the plane of rotation. The rotor configuration was designed to operate at a disk loading of 2.5 pounds per square foot and a tip speed of 540 feet per second. The values of the rotor solidity were 0.054 and 0.027 for the coaxial- and single-rotor configurations, respectively. The rotor blades had NACA four-digit

symmetrical airfoil sections and were of all-wood construction. The blades had a laminated birch spar and mahogany ribs and were covered with spruce plywood skin aft of the 22.6 percent chord. They were tapered both in plan form and thickness ratio but were untwisted. Details of the plan form and thickness ratio of the blades are presented in figure 1(a).

Another rotor (rotor 2) had been previously tested in the Langley full-scale tunnel. It was similar in design to rotor 1 except that it was rigidly restrained in flapping motion as well as in the plane of rotation. The blades were of all-metal construction, untapered in plan form, but tapered in thickness ratio. The values of the rotor solidity were 0.152 and 0.076 for the coaxial- and single-rotor configurations, respectively, and the rotor spacing was 2.0 feet (8 percent of the rotor diameter). Details of the plan form and thickness ratio of the blades of rotor 2 are given in figure 1(b).

A photograph of the general arrangement of the rotor hubs and drive mechanism of rotor 1 is shown as figure 2. The rotor drive was through a coaxial 7.4/1 reduction-gear box which turned the upper hub clockwise and the lower hub counterclockwise as viewed from above.

Rotor-blade pitch could be varied either collectively, differentially collectively, or cyclically. Collective pitch was obtained by changing the pitch of all the blades equally and in the same direction. Differential collective pitch control to provide directional control was applied by changing the pitch of the blades of the upper and lower rotors in opposite directions. Cyclic pitch control to provide rotor pitching and rolling control was applied by means of two feathering bearings mounted perpendicular to the drive shafts, one below each rotor, and connected by push-pull rods. All the controls were operated remotely by electric actuators and the control positions were measured by means of electrical bridge-type control position indicators.

A 266-horsepower motor mounted in a reaction-type dynamometer supplied the power to drive the rotor. Power input to the rotor was measured by a strain-gage beam so mounted as to resist the turning reaction of the motor casing. Rotor speed was measured by a standard aircraft tachometer.

The rotor and drive-motor combination was supported in a strain-gage balance which provided a direct measurement of the rotor thrust, pitching moment, rolling moment, and yawing moment. This balance was in turn mounted in trunnions which allowed the rotor to pivot about the center of the gear box so that the shaft angle of attack could be changed. The complete setup was mounted on the wind-tunnel balance by means of a diagonally braced 12-inch tube. In order to eliminate extraneous forces from the data, a free-floating sheet-metal fairing was

provided over the supporting members. Figure 3 is a photograph of the rotor as tested in the Langley full-scale tunnel.

The static-thrust investigation for both rotors was conducted for a range of rotor tip speed and blade pitch angle at zero shaft angle. Tests were made for both the coaxial- and single-rotor configurations in order to determine the relative merits of each. The static-thrust data were obtained with the longitudinal and lateral feathering controls neutral. For most of the coaxial tests the yawing moments were trimmed; however, some data were obtained with various amounts of preset directional control to determine the effect on rotor performance of unequal power input to the upper and lower rotors. All thrust data presented in this paper have been computed from the wind-tunnel-balance data.

RESULTS AND DISCUSSION

The results of full-scale-tunnel tests to determine the static-thrust performance of a coaxial rotor with blades tapered both in plan form and thickness ratio (rotor 1) are presented in figures 4 and 5. The variation of rotor thrust coefficient C_T with torque coefficient C_Q for both the coaxial-rotor ($\sigma = 0.054$) and single-rotor ($\sigma = 0.027$) configurations is presented in figure 4. Because of vibration the maximum tip speed of rotor 1 had to be limited to 500 feet per second. Data were therefore obtained for the coaxial configuration at several tip speeds to determine the scale effect on rotor performance. An appreciable difference in performance believed to be due to scale effect was noted for values of tip speed between 327 feet per second and 450 feet per second (fig. 4); the difference, however, became relatively small between 450 feet per second and 500 feet per second.

The hovering performance of rotor 1 was determined over a range of thrust coefficient from $C_T = 0$ to $C_T = 0.00557$ for the coaxial rotor and to $C_T = 0.00346$ for the single rotor at a tip speed of 500 feet per second. It appears that, within the experimental accuracy, the profile torque coefficient C_{Q_0} at $C_T = 0$ of the coaxial arrangement (0.0000777) was twice that measured separately for either of the single rotors.

The effect of variation in directional control (differential collective pitch, positive when added to the lower rotor and subtracted from the upper rotor) on the static-thrust performance of the rotor operating at a tip speed of 500 feet per second is shown in figure 5. The maximum available positive differential control setting of 3° 30' (upper -1° 45', lower 1° 45') and maximum negative setting of 1° 40'

(upper 0° 50', lower -0° 50') had only slight effect on the rotor performance; the average was about a 2-percent increase in C_Q for a given value of C_T, over the range tested.

The variation of rotor figure of merit M with the ratio of thrust coefficient to solidity C_T/σ for both the coaxial- and single-rotor configurations (rotor 1) is shown in figure 6. The maximum figures of merit were about 0.635 and 0.615 for the coaxial and single rotors, respectively. A comparison of these values with those predicted by rotor-hovering theory indicates that, within experimental accuracy, the difference in the figures of merit could be attributed to the difference in solidity of the coaxial- and single-rotor configurations.

In order to determine whether existing rotor-hovering theory was adequate to predict the hovering performance of a coaxial rotor based on a single-rotor analysis, a theoretical analysis of the hovering performance of both the coaxial- and single-rotor configurations was made by using the method described in reference 1. In this analysis the coaxial rotor was treated as a single four-blade rotor having the same solidity. The blade section characteristics were represented by the following formulas:

$$c_l = a\alpha_r$$

$$c_{d_o} = \delta_0 + \delta_1\alpha_r + \delta_2 a_r^2$$

where δ_0 is equal to c_{d_o} at $C_T = 0$ and δ_1 and δ_2 are determined from figures 2(b) and 2(c) of reference 2. Two-dimensional semismooth airfoil data, representative of the blade thickness ratio and Reynolds number at the 0.75 radius (x = 0.75) and a lift-curve slope a = 5.73, were used in the determination of δ_1 and δ_2. The calculated value of C_T was corrected for tip loss by assuming that the outer 3 percent of the blade span had no thrust but had profile drag. (This tip-loss factor is commonly used in rotor analysis (reference 2).) The results of the hovering analysis for both the coaxial- and single-rotor configurations are presented in figure 7. A comparison of these results with the measured test points indicates that, by assuming a single rotor of equal solidity, the hovering performance of a coaxial rotor, similar in blade geometry and rotor spacing to the rotor tested, can be predicted with the same degree of accuracy as that of a single-rotor configuration.

Some previously obtained full-scale-tunnel hovering-performance data for another coaxial rotor of similar spacing but entirely different blade geometry (rotor 2) were also available. Curves of the variation

of C_T with C_Q for both the coaxial- and single-rotor configurations and a plot showing the effect of variation in directional control on this coaxial rotor are presented in figures 8 and 9, respectively. These data indicate the same general trends as those for rotor 1.

The hovering performance of rotor 2, calculated in the same manner as was previously done for rotor 1, is shown in figure 10, and the same general agreement between experiment and theory as obtained for rotor 1 is shown.

The analyses made for rotors 1 and 2 indicate that the hovering performance of coaxial rotors having rotor spacings similar to those tested (8 percent to 9.5 percent of the rotor diameter) can be calculated with the same degree of accuracy as that of a single-rotor configuration by assuming a single rotor of equal solidity. However, it should be noted that an accurate knowledge of the zero-lift drag of the rotor is required for a reliable prediction of hovering performance.

CONCLUDING REMARKS

The following remarks are based on the results of Langley full-scale-tunnel static-thrust tests of a coaxial- and a single-rotor helicopter configuration having blades tapered both in plan form and thickness ratio.

1. The profile torque coefficient of the coaxial rotor operating at a tip speed of 500 feet per second was 0.0000777. Within the limits of experimental accuracy the profile torque coefficient of the single rotor was about one-half that of the coaxial rotor.

2. Variation in the directional control to the maximum available limits of $3^\circ\ 30'$ and $-1^\circ\ 40'$ resulted in about a 2-percent increase in torque coefficient over that of the trimmed rotor.

3. The maximum figure of merit measured for the coaxial rotor was 0.635 while that for the single rotor was 0.615. Calculations indicate that this difference is probably due to the difference in solidity of the two configurations.

4. The hovering performance of coaxial rotors having rotor spacings of the order of 8 percent to 9.5 percent of the rotor diameter can be predicted with the same degree of accuracy as that of a single rotor by assuming a single rotor of equal solidity for purpose of calculation.

Langley Aeronautical Laboratory
National Advisory Committee for Aeronautics
Langley Field, Va., December 28, 1950

REFERENCES

1. Gessow, Alfred: Effect of Rotor-Blade Twist and Plan-Form Taper on Helicopter Hovering Performance. NACA TN 1542, 1948.

2. Bailey, F. J., Jr.: A Simplified Theoretical Method of Determining the Characteristics of a Lifting Rotor in Forward Flight. NACA Rep. 716, 1941.

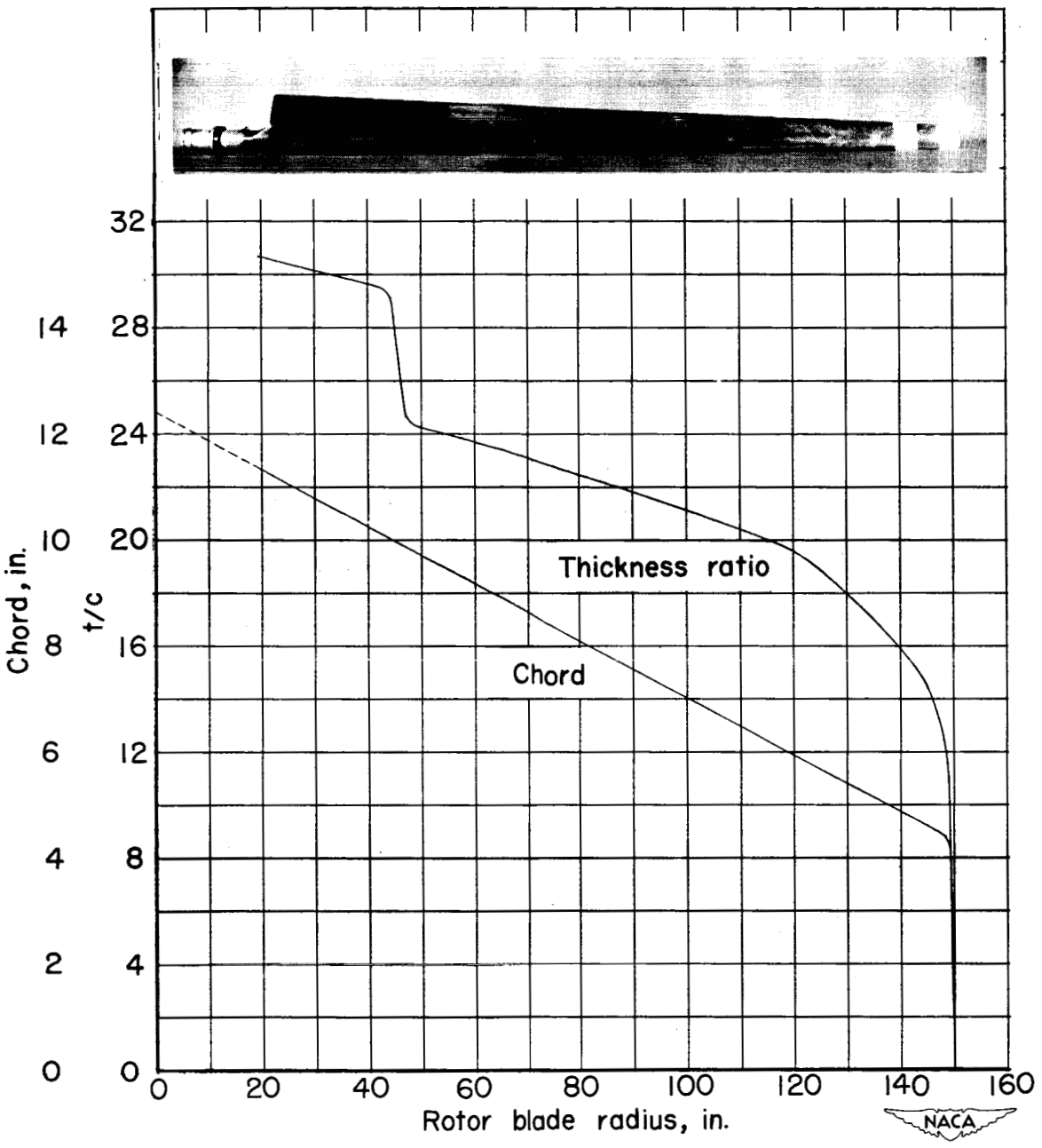

(a) Rotor 1.

Figure 1.— Variation of rotor blade chord c and thickness ratio t/c with blade radius r.

Page intentionally left blank

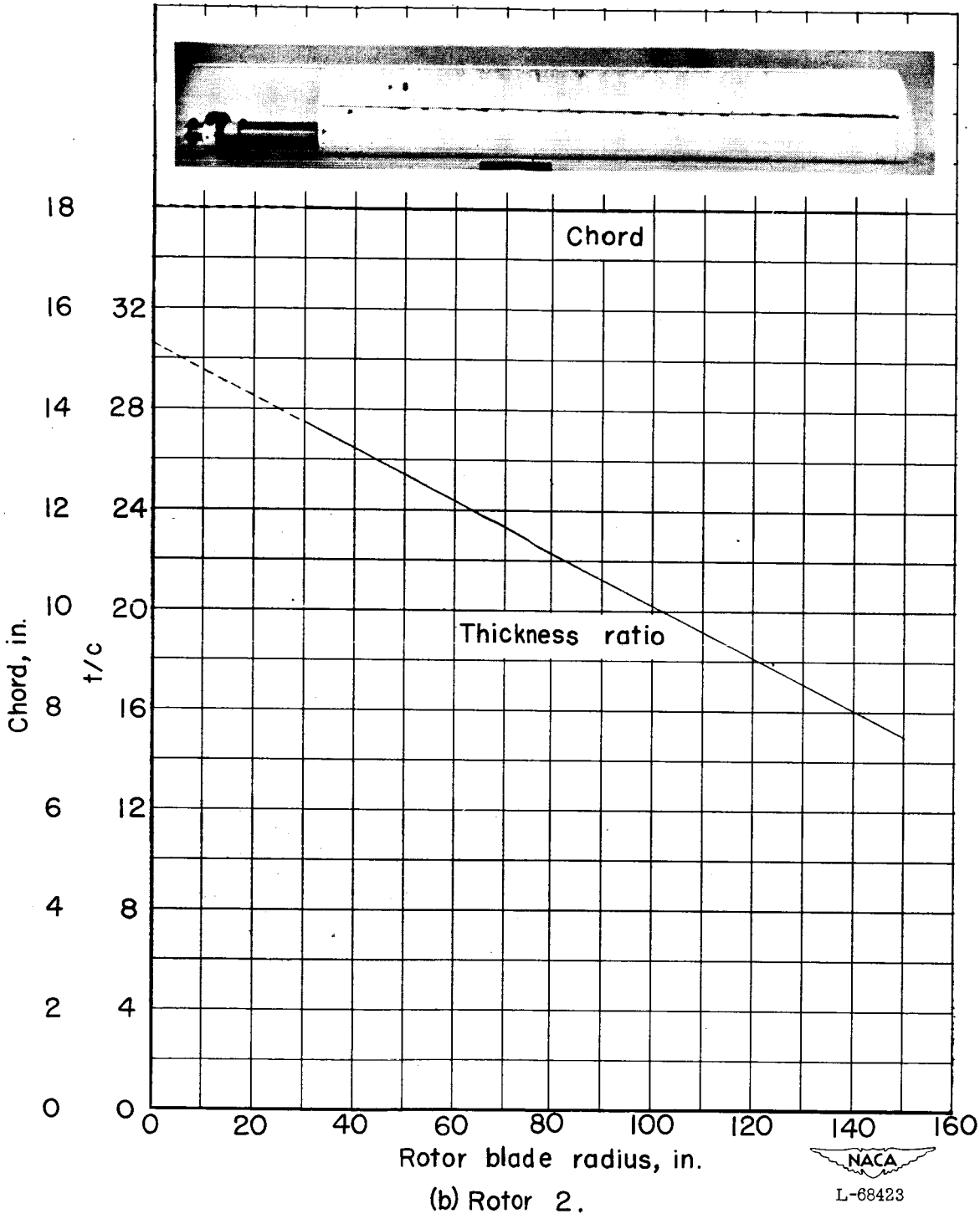

(b) Rotor 2.

Figure 1.— Concluded.

Page intentionally left blank

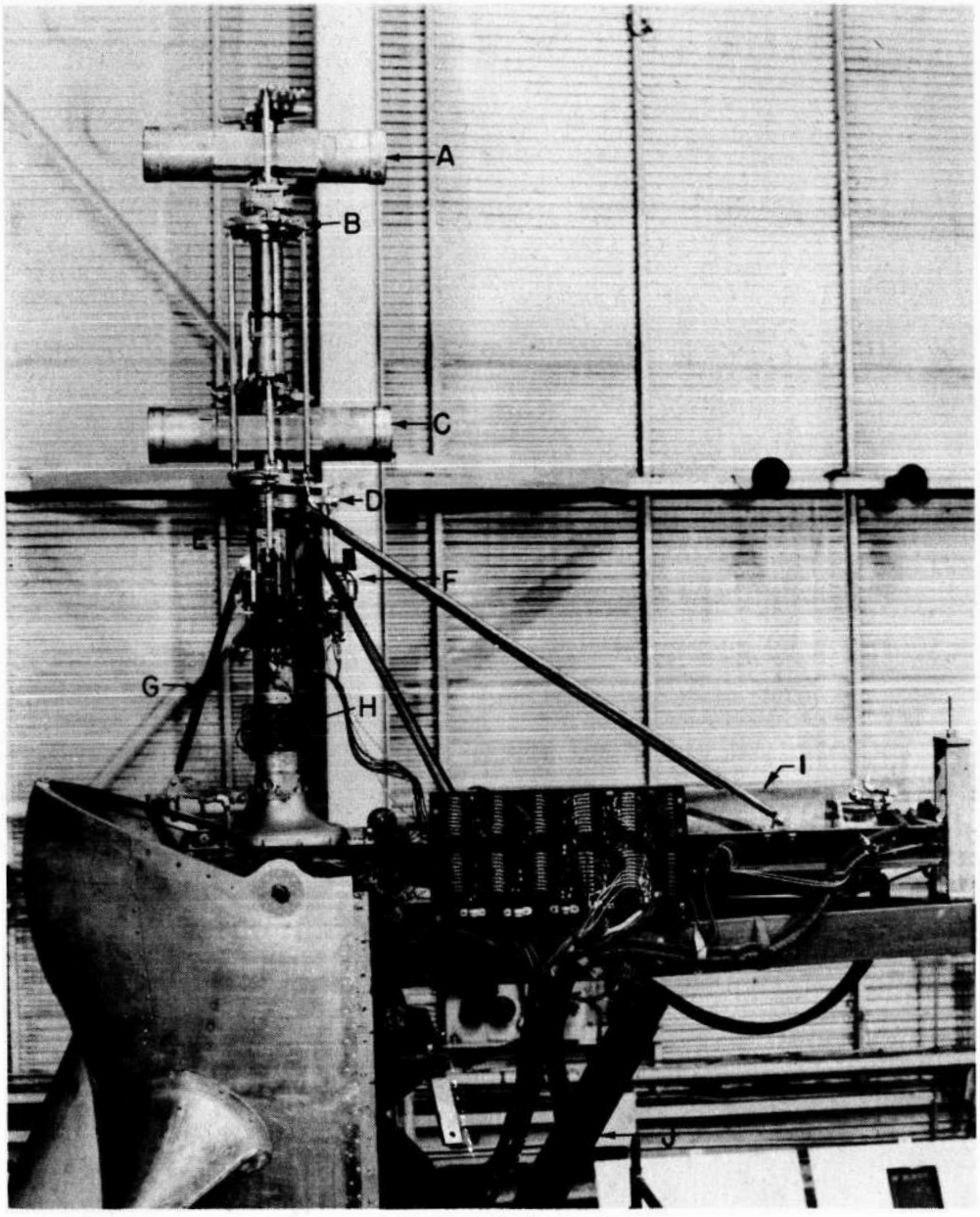

A Upper rotor hub
B Upper feathering bearing
C Lower rotor hub
D Lower feathering bearing
E Lateral feathering actuator
F Longitudinal feathering actuator
G Lower rotor collective-pitch control rod
H Lower rotor slip rings
I Drive motor
J Angle-of-attack arm

Figure 2.- General arrangement of the coaxial helicopter rotor (rotor 1) with the rotor blades removed.

NACA
L-65743.1

Page intentionally left blank

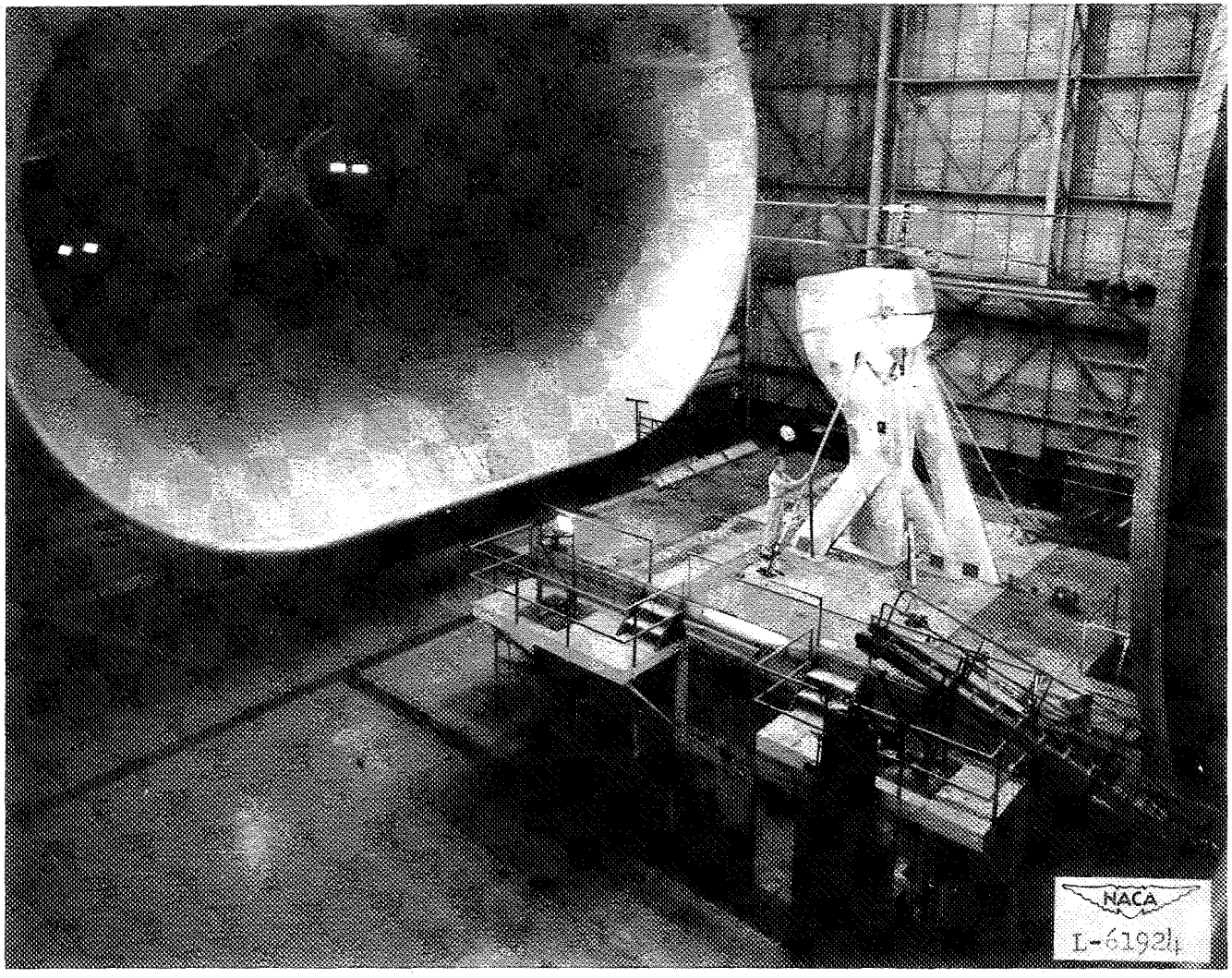

Figure 3.- General arrangement of the coaxial helicopter rotor (rotor 1) as mounted in the Langley full-scale tunnel.

Page intentionally left blank

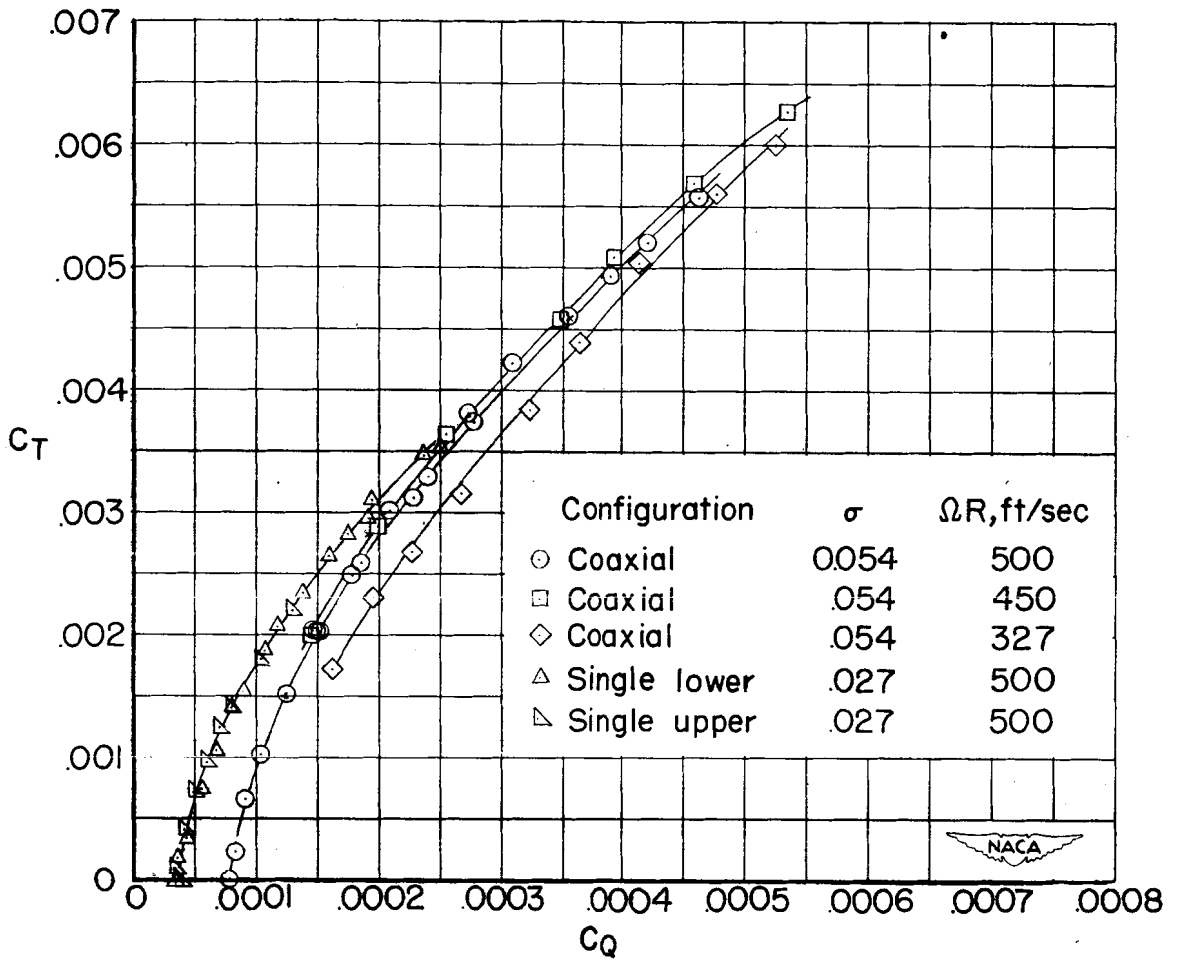

Figure 4.—Variation of thrust coefficient C_T and torque coefficient C_Q for a coaxial helicopter rotor (rotor I) in static thrust; yawing moments trimmed. c_r/c_t=2.92.

Preceding page blank

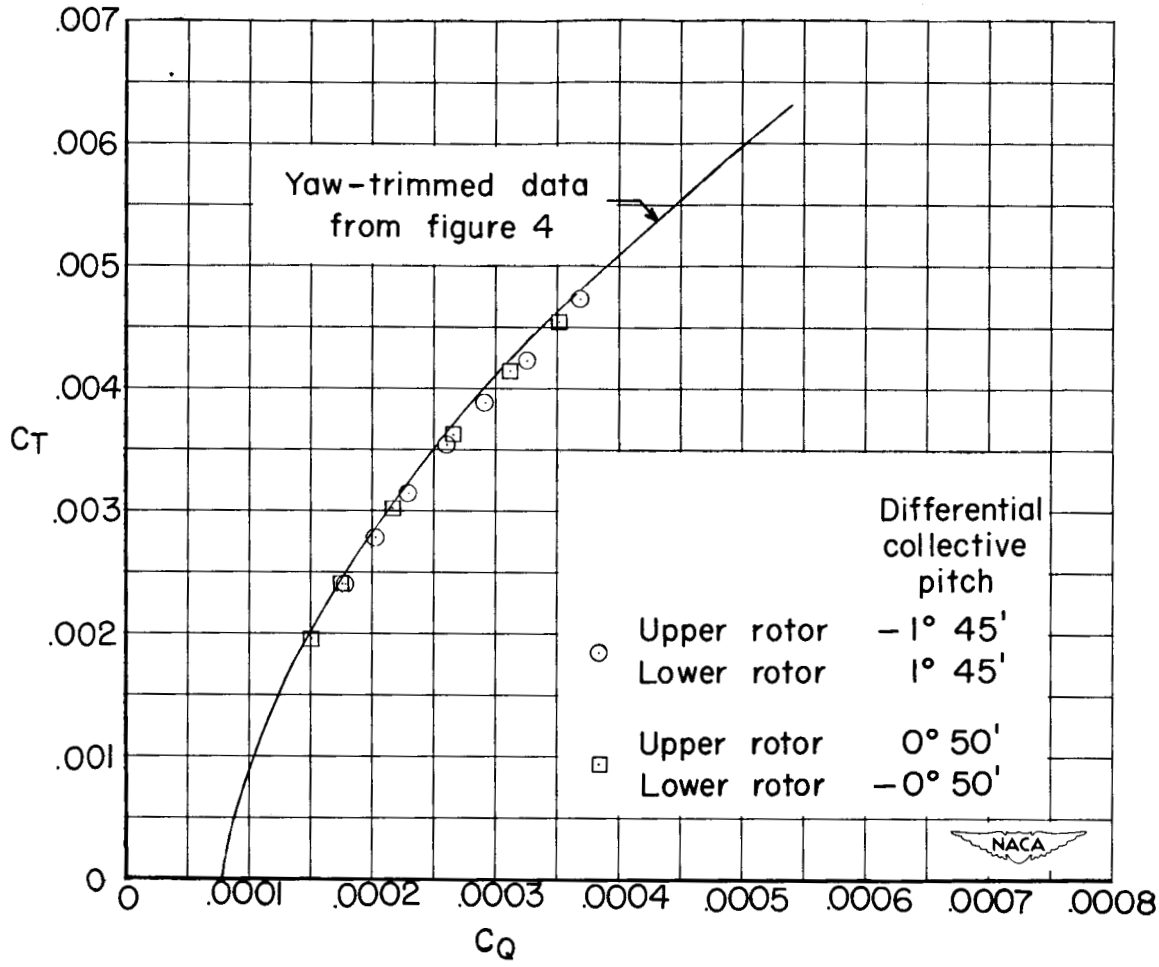

Figure 5.—Effect of variation in directional control on the static-thrust performance of a coaxial helicopter rotor (rotor 1); yawing moments untrimmed. $c_r/c_t = 2.92$. $\Omega R = 500$ ft/sec.

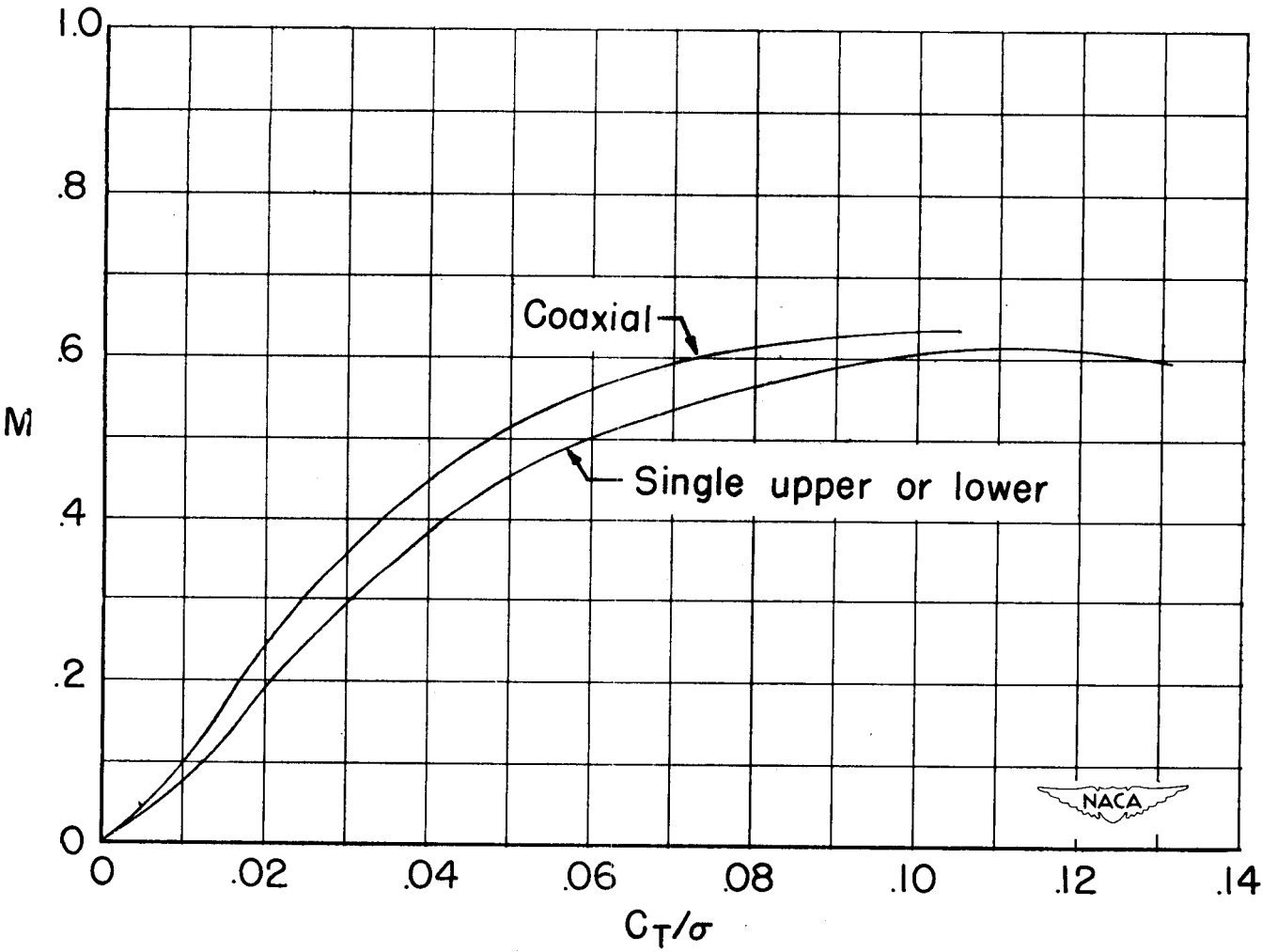

Figure 6.—Variation of rotor figure of merit M and thrust coefficient-solidity ratio C_T/σ for a coaxial and single rotor helicopter (rotor I) in static thrust. $c_r/c_t = 2.92$.

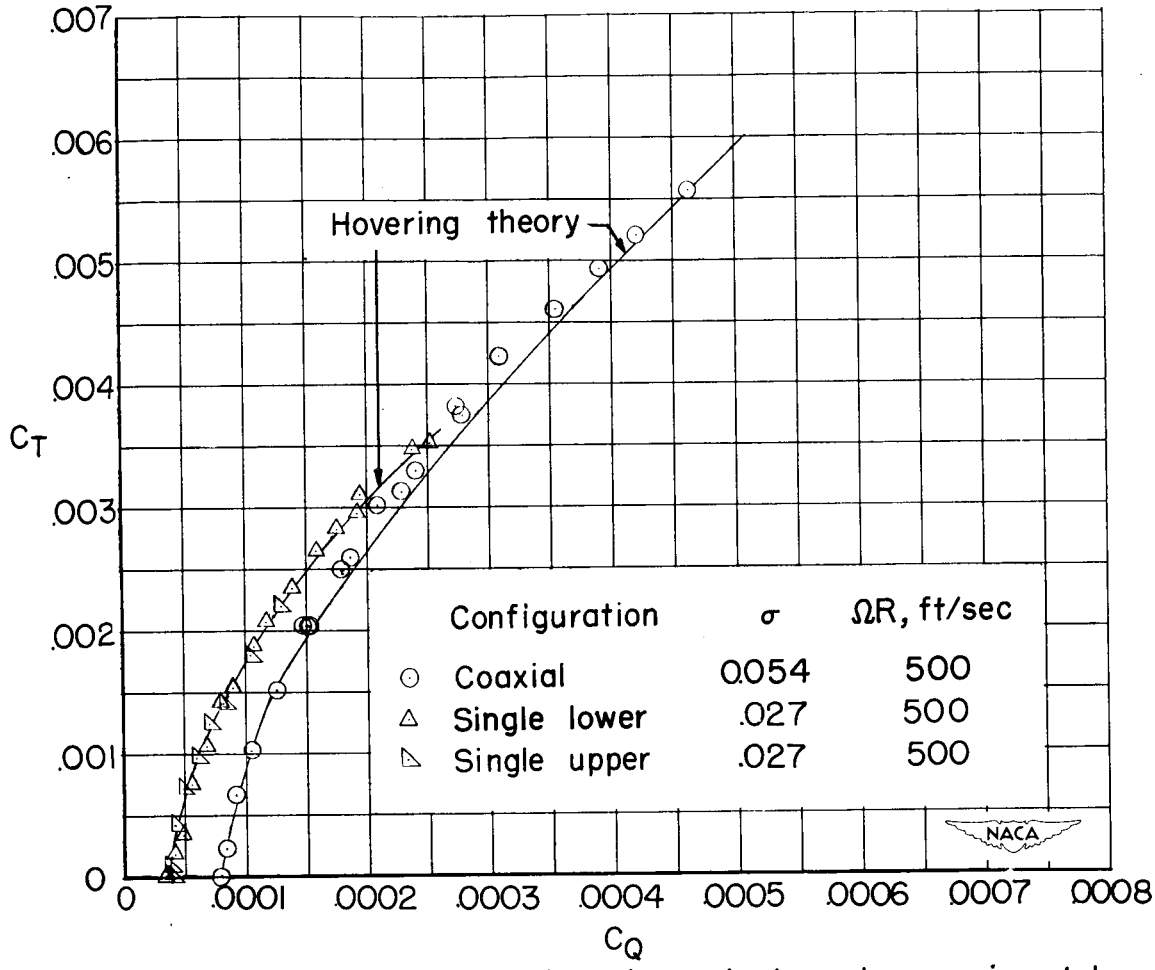

Figure 7.—Comparison of the theoretical and experimental static-thrust performance of a coaxial helicopter rotor (rotor 1) with blades tapered both in plan form and thickness ratio. $c_r/c_t=2.92$.

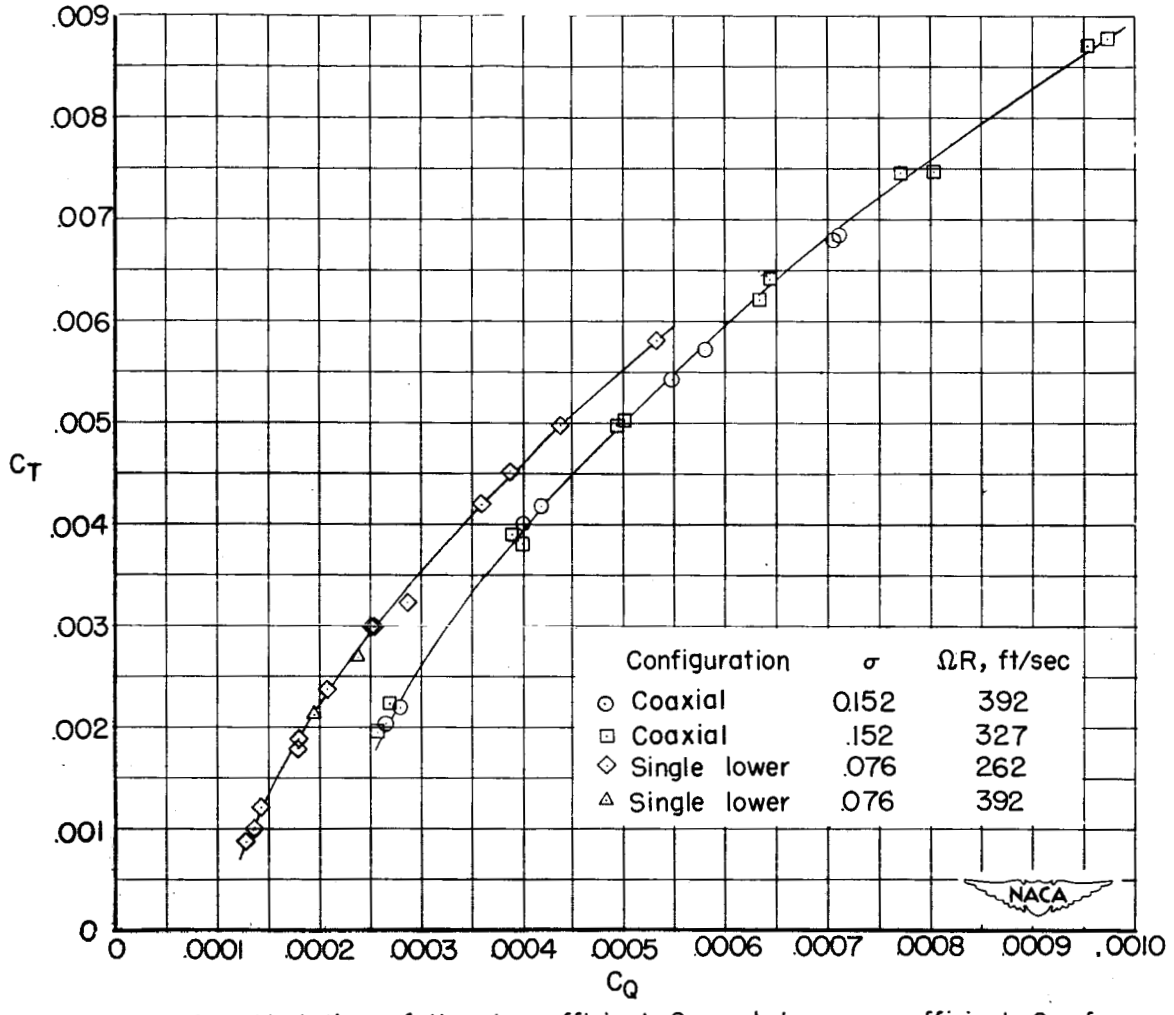

Figure 8.— Variation of thrust coefficient C_T and torque coefficient C_Q for a coaxial helicopter rotor (rotor 2) in static thrust; yawing moments trimmed. $c_r/c_t = 1$.

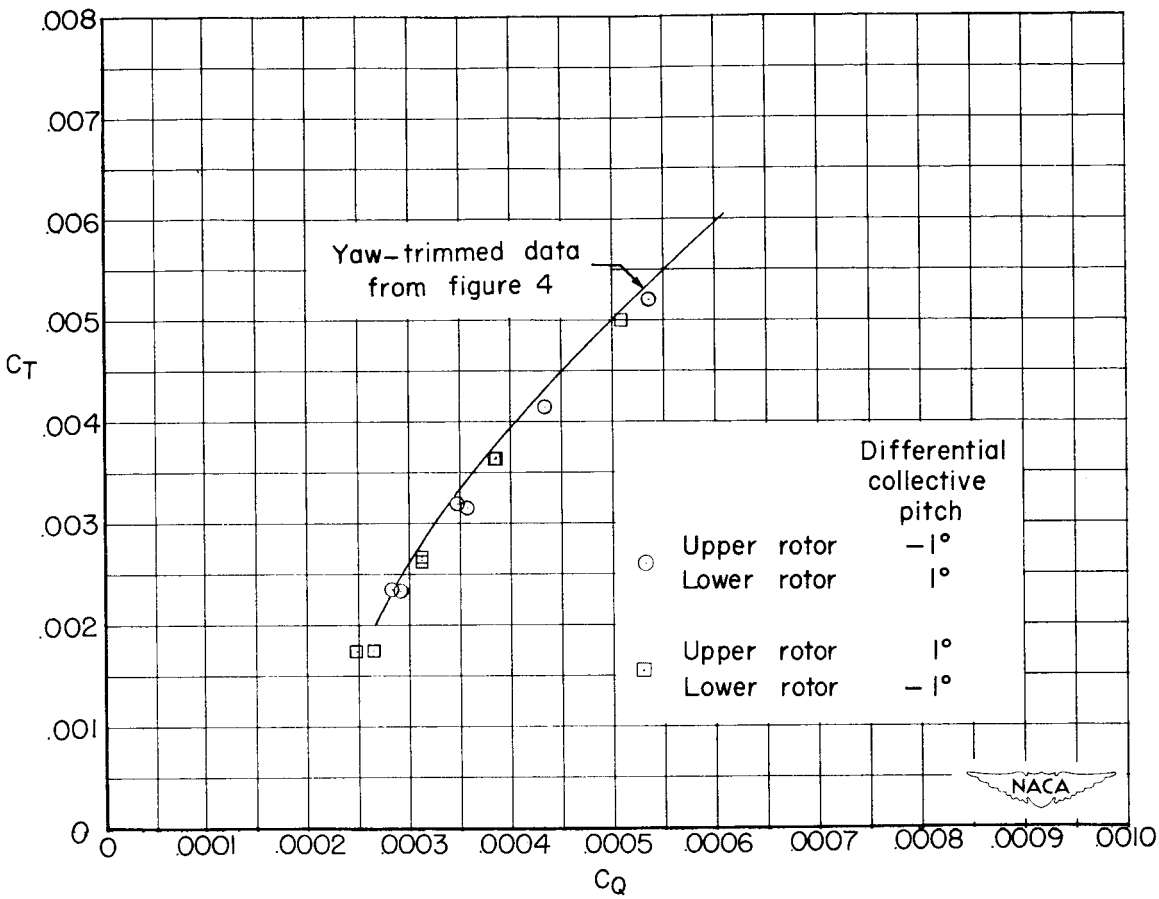

Figure 9.—Effect of variation in directional control on the static-thrust performance of a coaxial helicopter rotor (rotor 2); yawing moments untrimmed. $c_r/c_t = 1$. $\Omega R = 327$ ft/sec.

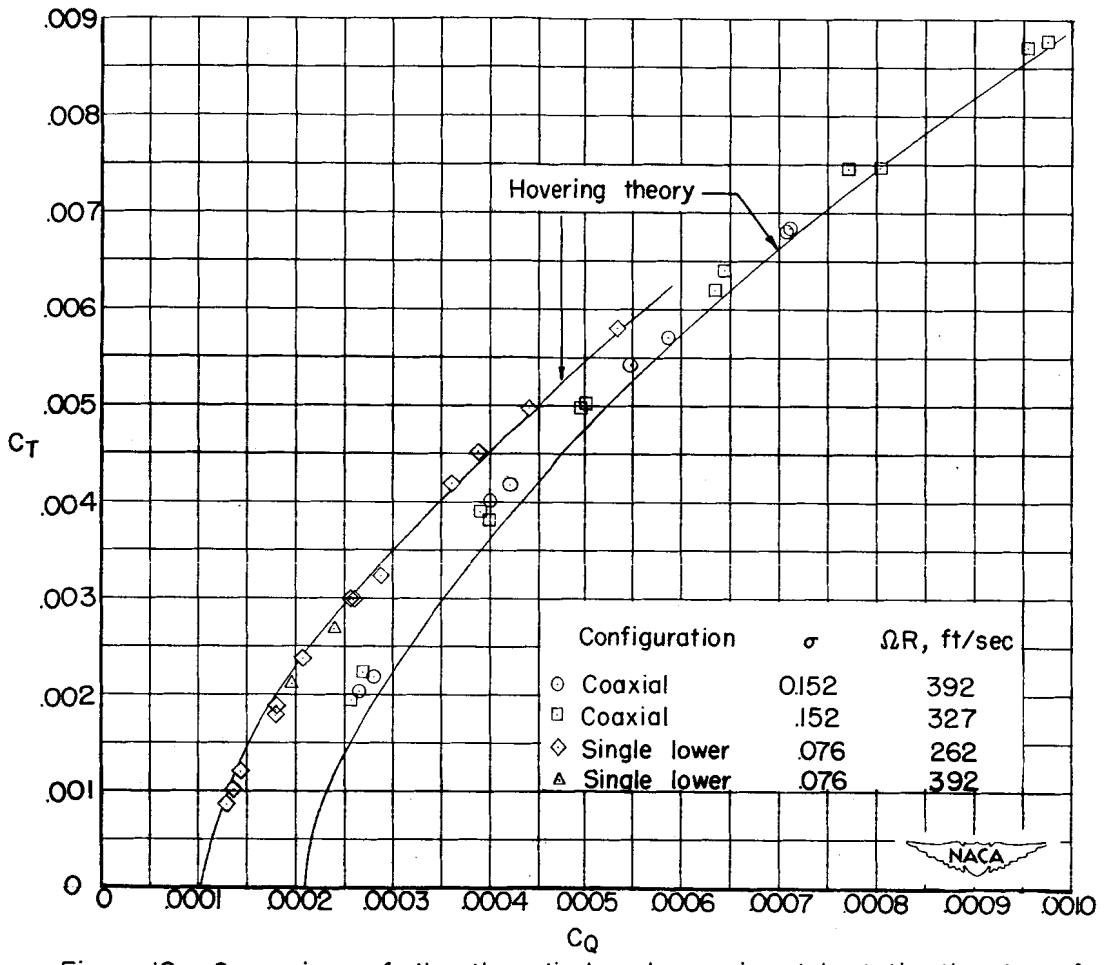

Figure 10.—Comparison of the theoretical and experimental static-thrust performance of a coaxial helicopter rotor (rotor 2) with blades tapered in thickness ratio only. $c_r/c_t=1$.